An analytical differential resistance pulse system relying on a time shift signal analysis – applications in Coulter counting.

Peter R. Birkin[a]*, Steven Linfield[a], Guy Denuault[a], Ronald Jones[b], Jack J. Youngs[a], and Emily Wain[a].

[a]Chemistry, University of Southampton, Southampton, SO171BJ, UK.

[b]Chemistry, University of Utah, Salt Lake City, Utah.

ABSTRACT: Improving the sensitivity and ultimately the range of particle sizes that can be detected with a single pore extends the versatility of the Coulter counting technique. Here, to enable a pore to have greater sensitivity, we have developed and tested a novel differential resistive pulse sensing (DiS) system for sizing particles. To do this the response was generated through a time shift approach utilising a 'self servoing regime' to enable the final signal to operate with a zero background in the absence of particle translocation. The detection and characterisation of a series of polystyrene particles, forced to translocate through a cylindrical glass microchannel (GMC) by a suitable static pressure difference using this approach, is demonstrated. An analytical response, which scales with the size of the particles employed, was verified. Parasitic capacitive effects are discussed, however, translocations on the ms timescale can be detected with high sensitivity and accuracy using the approach described.

The detection and characterisation of particles of various sizes poses a significant technical challenge. While many different detection systems have been developed (e.g. Coulter counting[1,2], light scattering[3] and mass displacement systems[4]), presented here is a novel approach with a good signal to noise ratio and sensitivity compared to direct measurement of the ionic current flowing through a pore. In order to test the validity of this approach, a set of Coulter counter experiments were performed. This choice was driven by the characteristics of the Coulter[5] counting technique as it relies on a relatively simple principle that a particle entering a small channel effectively reduces the ionic pathways[6] through the conduit (through a simple volume displacement principle) and results in a loss in ionic conductivity of the structure[7]. This principle has been effectively used to study nanoparticle[8] translocation through nanopores[9–11] and the passage of DNA strands through a structure[12–14]. The latter of these two has enabled the development of highly sophisticated DNA sequencing stratergies[15,16]. Dynamic and tuneable pores have also been reported[17]. While these eloquent examples exist, one fundamental limitation is the range of particle sizes that a particular channel can sensibly detect against the overall current and the inherent background noise. Clearly it is desirable to use a system which is dynamic (i.e. can detect fast moving particles), sensitive (i.e. can detect as wide a range of particles as possible) and versatile (i.e. can be applied to many systems). To increase the sensitivity of the technique, several different strategies may be employed. These could include the fabrication of bespoke channels[1,10,18] either in glass[19–21] or other insulators. Such approaches can give systems the ability to sense rapid translocation frequencies. For example Fraikin *et al.* used a bridge configuration with a sensing electrode placed between constrictions to detect up to 5 x 10^5 particles per second[22]. Alternatively, the sensitivity of the experimental apparatus, which enable the detection of small changes in ionic conductance through the channel to be monitored, could be improved and combined with bespoke channels[7,23,24]. This combination will enable the most versatile system, in terms of particle sizing, to be developed. In this latter category, differential systems have been reported[25]. These typically operate by measuring the ohmic changes[7] that occur as a particle translocates through a channel using electrodes placed either side of a suitable conduit and connected to the differential inputs of an operational amplifier, for example. This approach has been successfully adopted for the detection of small particle translocation through channels. While this is useful, other strategies can be adopted. The approach presented here (and in particular the circuit developed) attempts to address two fundamentally opposing limitations of dynamic range and sensitivity. This is achieved by implementing the novel approach of separating the signal into two paths: a "fast" path (which appears as a step function) and a "slow" path (which appears as the same step function but with a reduced bandwidth). These two signals are subtracted and the result, after appropriate amplification, recorded. This approach is somewhat reminiscent of a classical PID controller[26] that combines a proportion, an integrated and a differentiated signal to derive an error voltage. In the case reported here, the signal from a GMC is measured against a dummy resistor in a bridge configuration. The characterisation of this system is reported with the use of polystyrene monodispersed beads driven through the GMC using a suitable pressure difference. This simple system was chosen to highlight the function and advantages of the time shift approach we describe.

EXPERIMENTAL

The GMCs used in this work were fabricated by sealing copper microwire (40-64 μm diameter, Advent Research Materials) into soda glass (~2 mm OD) capillaries using a flame. These structures were polished with fine emery paper followed by 1 μm and 0.3 μm alumina (Struers) on polishing clothe (Buehler) to a mirror like finish. The exposed wire template was then etched with a mixture of HCl/H_2O_2 (Care). The final dimensions of the pores where determined by measuring their resistance using conventional cyclic voltammetry in an electrolyte solution (see Figure S1) and also by optical inspection of the structure using a Navitar x12 lens and Jai camera. Figure 1 shows images of the resultant structures produced in this fashion. The translocation experiments were performed using a two-electrode arrangement whereby Ag/AgCl electrodes (Ag wire electrodes, Advent Research Materials, anodised in chloride media), were placed either side of the pore. Solutions (0.1 mol dm^{-3} KCl, Fisher, 99%) were driven through the pore using a static pressure differential. This pressure ensured fast translocation (< 2 ms) and avoided any significant electrokinetic effects. The exact

pressure difference with respect to atmospheric pressure was measured using an EBRO vacuum meter VM 2000 and is reported in the appropriate figure legend. Note that the hydrostatic head will result in a 1.5 kPa loss in pressure differential across the GMC itself in all experiments. Figure S2 shows a schematic representation of the rig used. The apparatus was contained in a Faraday cage in an effort to reduce electrical noise. Translocation events where measured for a variety of different physical parameters on a series of polystyrene particles (here 11.1 ± 0.25 µm and 18.8 ± 1.2 µm diameters – manufacturer supplied data).

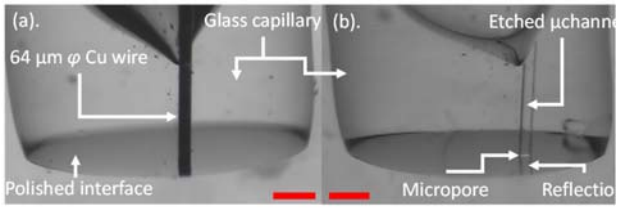

Figure 1. Images of a sealed wire and pores such as those used in this study. (a) shows a side view where a 64 µm diameter Cu microwire has been sealed in 2 mm OD soda glass capillary tubes while (b) shows an image of the etched pore (GMC). In each case the scale bar represents 200 µm.

Solutions containing particles were made from the suspensions supplied by the manufacturer (Polysciences) and diluted in 0.1 mol dm^{-3} KCl to the appropriate sphere concentration (typically 7.1 x 10^4 cm^{-3}) by weighing out the particle stock solution once it had been ultrasonicated and then vortex mixed (Fisher brand) for a period of ~ 30 s per treatment. The translocation events were measured in two ways; using the current passed through the pore or a differential signal both recorded as a function of time. In the first case this involved the use of a simple current follower and DC supply, while in the second a differential signal was generated using a bespoke piece of apparatus. This was designed and constructed in-house from PCBs fabricated by a professional board house (PCBway.com). The circuit diagram is shown in figure S3. The signals obtained from this approach were recorded on a 16 bit DAQ card (USB1608FS Plus, Measurement Computing (sampling data up to 100 kHz but typically 10 kHz was employed) interfaced using

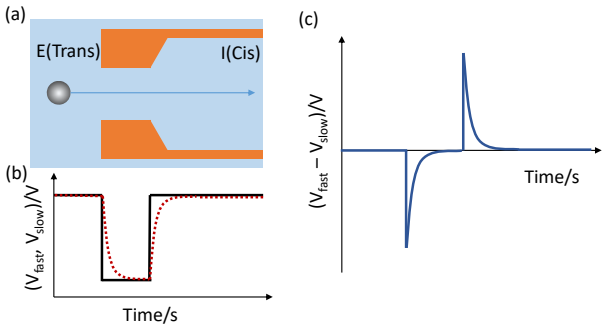

Figure 2. (a) a schematic representation of the particle (●) translocation through a microchannel (▮) from the exterior (E) to the interior (I). (b) the measurement of the sensing voltage (V_s) split into two pathways, a fast (V_{fast}, —) and a slow (V_{slow}, ▪▪▪) route. (c) the signals are subtracted to give the differential pulse (—).

VS2010 (Microsoft) and Measurement studio (National Instruments) software. All solutions were made with aerobic purified water (18.2 MΩ cm, Purite Select Fusion system) at 20-25^{0}C.

RESULTS AND DISCUSSION

The concept deployed here is to exploit a simple series resistor bridge involving two components; the first is a dummy resistor (*R*d) while the second is the micropore (*R*p). The mid potential of the system (with a DC bias placed across the resistor pair) is then measured (see figure S3). If this DC bias was simply amplified, the process would produce a significant voltage which could cause instrument saturation. Also, small and unavoidable DC drift would skew the results. To avoid this problem of saturation, plus DC offset and drift, we take the novel approach by sending the mid potential through a circuit which essentially has two paths, one to capture high frequency components (here termed "fast") and a second path

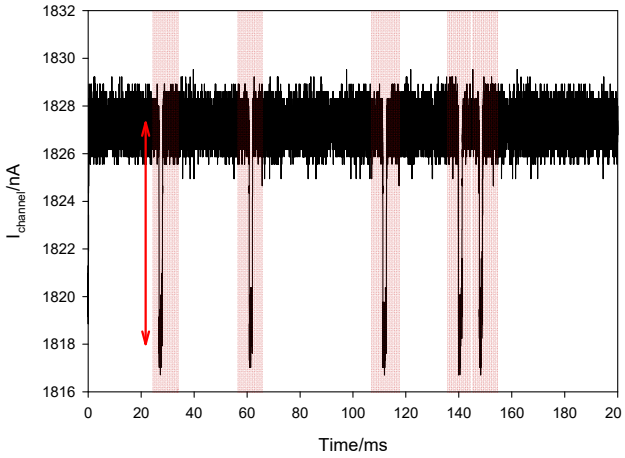

Figure 3. Plot showing the current as a function of time for 18.8 µm diameter particles translocating through a 40 µm diameter pore (—). Here a potential of 1 V was applied between the two Ag/AgCl electrodes. The solution contained 7.2 x 10^4 particles cm^{-3} in 0.1 KCl. A pressure differential of 77 mbar was applied to drive the translocations. The highlights (▮) show the positions of the translocations and the theoretical change[2,27] is shown as a red arrow.

that captures lower frequency components (or "slow"). These fast and slow signal pathways are then subtracted from one another. The resultant signal can then be amplified and appears like a differential pulse, the exact shape of which is determined by the shape of the resistance change as a result of a particle translocation and the experimental performance of amplifiers employed. The differential signal can then be amplified (to give V_a) and measured. Figure 2 shows a schematic of this approach. While this approach will work, some refinement is necessary. Non-ideal performance in the circuit (specifically the amplifiers) often result in small offsets being included in the resultant signal. These, when amplified (note we amplify by up to 10^4 V/V), cause significant DC offsets. In order to avoid these a second 'self-servo' section of the apparatus was conceived and implemented. Here a second low pass filter with a cut off frequency ~20 times lower (selected through simulation of the complete circuit, ADISimPE) than the first was utilised. The signal from this stage (V_{pss}) can then be subtracted from the post amplified stage (V_a) to give the final voltage, V_{DiS} (i.e. $V_{DiS} = V_a - V_{pss}$). This approach ensures that the resultant signal remains centred at 0 V in the absence of a translocation event. Figure S4 shows a schematic of the complete approach adopted. In order to test the functionality of this approach, particle translocations

through a GMC, driven by a suitable stable pressure gradient, were investigated. Figure 3 shows the signal obtained from such a system. In this case the current flowing through a 40 µm diameter GMC was monitored as a function of time when a 1 V bias was applied between the interior (I) and exterior (E) compartments employed. Under these conditions, the current should vary by ~ 0.54 % as an 18.8 µm diameter polystyrene microsphere translocates through the GMC. This change was calculated using the appropriate formula[28,29] for conventional Coulter counter analysis and is included in figure 3 as an arrow. There is good agreement between the transients observed for the 18.8 µm diameter spheres translocating through the 40 µm diameter GMC. The translocation events were found to be on the order of 1.4 ms in duration. However, the signal to noise under these conditions is non-ideal (S/N ~ 5 for a current change of ~9.4 nA for an 18.8 µm translocation *vs.* 1.8 nA zero-to-peak noise).

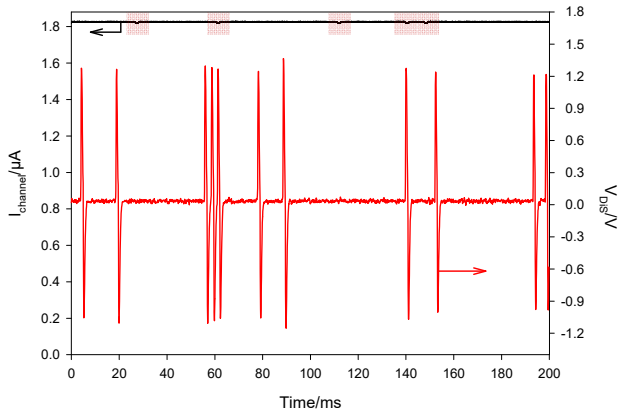

Figure 4. Plots showing the current through a GMC ($I_{channel}$, —) and a V_{DiS} signal (—) obtained using the approach outlined in the text. In both cases a 40 µm pore was used. The solution contained 18.8 µm polystyrene particles. A bias of 1 V and 2 V for the current follower and resistance DiS system was applied respectively. Note the highlights on the current time signal ( ) show position of particle translocation.

This will decrease significantly for smaller particles (e.g. an estimation of an S/N~ 1 for a current change of 1.9 nA for a 11.1 µm diameter particle translocation *vs.* 1.8 nA zero-to-peak noise, see figure 3). If the same 18.8 µm particles are translocated through the same GMC but monitored using the differential resistance pulse (DiS) approach, a significantly higher signal to noise ratio was observed. Figure 4 shows the translocations detected using the differential system (—), here a signal to noise ratio of ~50 was recorded (1.2 V *vs.* 0.024 V zero-to-peak for the particle translocation and the noise respectively in this case, note we ignore the particle leaving the channel in this case). This is compared to the S/N of ~5 for the current follower method. This represents an order of magnitude improvement compared to the conventional current follower signal (—) which is included in figure 4 and plotted versus 0 nA for a suitable comparison. While, it would be possible to filter the current time data to improve sensitivity, this is not without consequences. For example, this will limit the temporal resolution of the system and, as a result, restrict the translocation times that can be studied without distortion. Several further points should be noted. First, two transient signals are apparent per translocation event. This is caused by the particle entering (here shown as a positive potential transient) followed by the particle leaving the GMC (shown as a following negative potential transient). The positive and negative transients result in an effective doubling of the signal compared to the conventional current transients. Second, the events are centred on zero volts as a result of the self-servo approach employed (see SI for further discussion). The amplitudes of the positive transients can be used to calculate the size of the particles involved. Under the conditions employed, the size of the positive transient can be shown (see SI data) to be,

$$V_{DiS} = \frac{V_{ap} R_d G \Delta R}{\xi \theta^2} \qquad (1).$$

where ΔR is the change in resistance caused by the particle entering the pore, θ is the sum of the dummy resistance, R_d, and the pore resistance, R_p, V_{ap} is the applied voltage, ξ is the instrumentation sensitivity factor, G the amplifier gain (typically 10^3 V/V) and V_{DiS} the output voltage. The output voltage should be dependent on the overall applied voltage V_{ap}. This was found to be the case (see SI, figure S5). Note that the incorporation of the instrument sensitivity factor is a direct result of the performance of the amplifiers employed and other non-ideal behaviour (for example the parasitic capacitance of the cables employed, the amplifier inputs and PCB tracking). In order to account for these factors, the response of a dummy cell was measured (see figure S6) and the correction factor

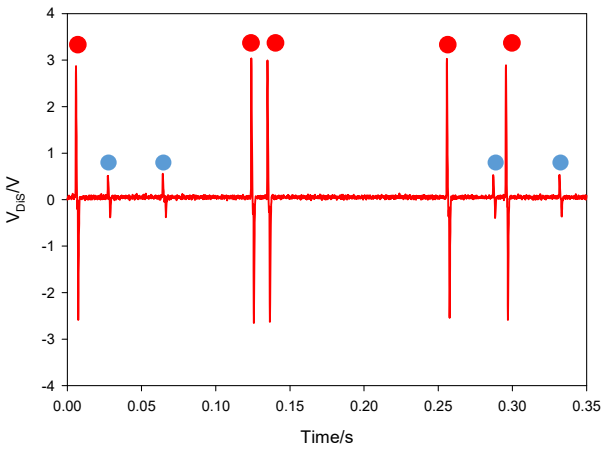

Figure 5. Plots showing the DiS signal (—) obtained from a 40 µm pore placed in a 0.1 M KCl solution contained 18.8 µm and 11.1 µm diameter polystyrene particles. A bias of 5 V was applied across the pore and dummy resistor (1 MΩ). Note the highlights on the signal (●, ●) show particle translocations attributed to single 11.1 µm, 18.8 µm events respectively. A pressure differential of 54 mbar was applied across the system.

included as appropriate in all subsequent data analysis. Figure 5 shows the response of a 40 µm diameter GMC placed in a solution containing both 18.8 µm and 11.1 µm polystyrene microspheres. In this case two clear types of transient (marked with different coloured circles) where observed, the magnitude of each being significantly different as expected. These are caused by the 18.8 µm diameter spheres (●) and 11.1 µm diameter spheres (●) translocating through the GMC. Figure 5 shows that the magnitude of the V_{DiS} signal is significantly different for the two particles indicating that the sizing resolution of the technique remains.

If the response of this 40 µm diameter GMC was monitored in this solution for a significant period of time (100 s), a large number of translocations (~3000) were detected. Selecting the maxima of each of these events (using a software routine based on National Instruments peak finding routine) and employing equation 1, the value of the change of resistance with respect to the resistance of the pore can be determined. Figure 6 shows the event frequency (▇) plotted against $\Delta R/R_p$. Included in this plot is the integral of the event count and an estimation of the predicted range expected for each particle employed using the conventional Coulter counter theory[28,29]. Figure 6 shows that there is good agreement between the predicted values

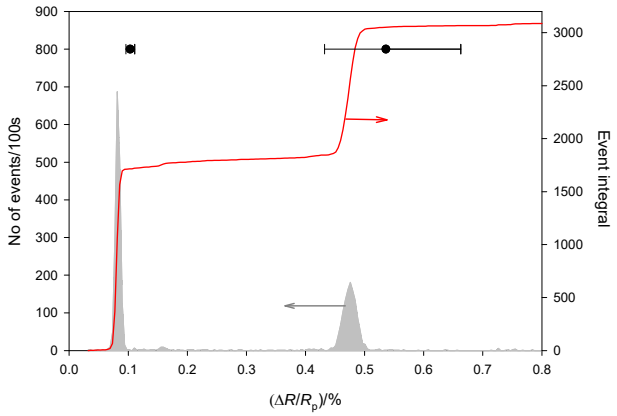

Figure 6. Plots showing the event count (▇) and the integral of the event count (▬) as a function of *ΔR/Rp* obtained from a 40 µm pore placed in a 0.1 M KCl solution contained 18.8 µm and 11.1 µm diameter polystyrene particles. The black circles (●) show the estimated values considering the particle size and the appropriate formulae[28,29]. The error bar shows the spread in the data estimated from the standard deviation of the particle sizes given by the manufacturer. All other conditions are as reported in figure 5.

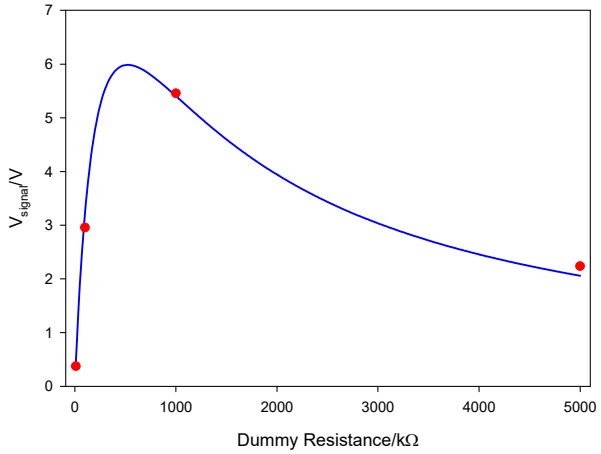

Figure 7. Plots showing the predicted response (▬) from a 40 µm pore placed in a 0.1 M KCl solution containing 18.8 µm diameter polystyrene particles as a function of the dummy resistor deployed. The red circles (●) show the experimental values corrected for instrumentational response. A pressure differential of 73 mbar was applied across the system and a bias of 5 V applied to the pore/dummy cell system. Note the predicted response was calculated for the 1 MΩ system and will not be 100 % accurate across the whole range (see SI data).

and the detected event height. In addition the spread of the data agrees with the associated magnitude of the data provided by the manufacturer for each of the polymer spheres employed although the 18.8 µm system appears narrower than expected. However, this is solely based on the data provided by the manufacturer and not confirmed by independent means. This validates the approach adopted and suggests that it can be used to gather useful information on the size of translocating particles through these pores. The system presented here uses a voltage divider approach to the measurement problem associated with a translocation (and hence resistance change) of a particle through a GMC. This was chosen for several reasons. First, it is a relatively simple approach. Second, it is inherently quiet in terms of electrical noise. This is a direct result of the components themselves (the resistors) as they produce relatively little noise under these conditions. Figure 7 shows how the predicted response (▬) of the system varies with the choice of the dummy resistor with maximum sensitivity gathered when the dummy resistor and the pore resistance are equal as expected. Here the predicted response (taking into account the instrument sensitivity factor) is compared to the experimental results (●) for particle translocation. Figure 7 shows that there is excellent agreement between the predicted response and the experimental data and that if the resistance of the dummy resistor is greater or less than the pore, then the sensitivity of the system drops away. Hence to attain the best sensitivity using this approach, matching the pore and dummy resistor resistances is desirable. This could be achieved through judicious choice of the dummy resistor employed in the circuit, altering the pore dimensions or even the salt concentration employed in the cell. However, this resistor bridge strategy does produce some limitations. For example, parasitic capacitance can be an issue in this system (see SI).

While the data presented here is clearly accurate and the technique has been shown to have analytical potential in this arena, some thought as to other advantages is pertinent. For example, a clear improvement on conventional current sensing strategies (in terms of signal to noise ratio) has been demonstrated (e.g. 50 *vs.* 5 for the V_{DiS} and current follower measurements respectively under these conditions). This will have implications for the detection limit of the particle size possible for a given pore. Consider the case where the pore dimensions are as those used in Figure 6 (e.g. 40 µm diameter channel with a base resistance of ~ 524 kΩ in 0.1 mol dm^{-3} KCl) is tested. Under these conditions, it is possible to calculate that for an S/N ratio of 1 (e.g. a 48 mV zero-to-peak signal) the particle diameter would be 4.7 µm using a 1 MΩ dummy resistor. This is approximately 1 order of magnitude lower than the pore diameter itself. However, if the length of the channel is reduced so that the 40 µm diameter GMC has a base resistance of 52.4 kΩ and the dummy resistor is matched (to allow for the maximum sensitivity of the measurement instrument, see figure 7) then the detection limit can be calculated to be 1.9 µm. However, some care should be applied here as simple reduction of the pore length, although illustrative, may have limitations associated with the function of the Coulter counter approach itself (and end effects) and would need further careful consideration. In addition this calculation does not take into account limitations of eq. 1 which have been discussed in the SI. Nevertheless, further refinement of the pore etc., including reducing the dimensions, may drive down the minimum size of particle possible to be detected using this approach. While this is clearly possible (and is exploited using glass nanopores[1], for example), it is beyond the current study and is the subject of further investigation.

Finally, if the electrical noise can be kept to a minimum (an inherent issue with systems that rely on differential analyses), this measurement approach could be used for other systems and is not just restricted to particle translocation. For example, the direct measurement of stochastic current[30–32] events or transient potential

signals, could be directed into this DiS system in efforts to improve the sensitivity of those measurements.

CONCLUSIONS

The DiS system presented here has been shown to be sensitive and useful for the analytical characterisation of particles translocating through a GMC. The signal to noise ratio of the system is one order of magnitude greater than conventional current sensing approaches enabling particle diameters a factor of ~10 smaller than the pore to be detected under the conditions employed. The system can measure rapid translocations (on the 1 ms timescale) and the sensitivity of the device, although limited by parasitic capacitance effects, is dependent on the resistors used (in relation to the pore resistance) and the applied voltage.

ASSOCIATED CONTENT

Supporting Information Available: The following files are available free of charge.

Birkin et al SI for ACS sensors.pdf. A document containing the SI data and discussion relevant to the main manuscript. This contains iV response of a pore, schematic representation of the experimental setup, circuit diagram of the instrument, signal handling approach, experimental data relating to voltage dependence of the response of the DiS system, derivation of the response *vs.* experimental parameters of the system, calibration data, the effect of parasitic capacitance and the response time of the system.

Keywords: Translocation, Coulter, Differential, Microchannel, Sensitivity

AUTHOR INFORMATION

Corresponding Author

*prb2@soton.ac.uk, Chemistry, University of Southampton, Southampton, SO171BJ, UK.

Author Contributions

The manuscript was written through contributions of all authors.

ACKNOWLEDGMENT

The authors would like to thank the Chemistry department at University of Southampton for support and Professor Henry White (University of Utah) and his group for useful discussions.

REFERENCES

(1) Luo, L.; German, S. R.; Lan, W.-J.; Holden, D. A.; Mega, T. L.; White, H. S. Resistive-Pulse Analysis of Nanoparticles. *Annu. Rev. Anal. Chem.* **2014**, *7* (1), 513–535. https://doi.org/10.1146/annurev-anchem-071213-020107.

(2) DeBlois, R. W.; Bean, C. P. Counting and Sizing of Submicron Particles by the Resistive Pulse Technique. *Rev. Sci. Instrum.* **1970**, *41* (7), 909–916. https://doi.org/10.1063/1.1684724.

(3) Panáček, A.; Kvítek, L.; Prucek, R.; Kolář, M.; Večeřová, R.; Pizúrová, N.; Sharma, V. K.; Nevěčná, T.; Zbořil, R. Silver Colloid Nanoparticles: Synthesis, Characterization, and Their Antibacterial Activity. *J. Phys. Chem. B* **2006**, *110* (33), 16248–16253. https://doi.org/10.1021/jp063826h.

(4) Nidhi, K.; Indrajeet, S.; Khushboo, M.; Gauri, K.; Sen, D. J. Hydrotropy: A Promising Tool for Solubility Enhancement: A Review. *Int. J. Drug Dev. Res.* **2011**, *3* (2), 26–33. https://doi.org/10.1002/jps.

(5) Coulter, W. H. Means for Counting Particles Suspended in a Fluid. *U.S. Pat.* **1953**, No. 2,656,508, 9.

(6) Rayleigh, Lord. Rayleigh 1892 4 Phil Mag.Pdf. *Philos. Mag.* **1892**, *34* (211), 481–502.

(7) Harms, Z. D.; Haywood, D. G.; Kneller, A. R.; Selzer, L.; Zlotnick, A.; Jacobson, S. C. Single-Particle Electrophoresis in Nanochannels. *Anal. Chem.* **2015**, *87* (1), 699–705. https://doi.org/10.1021/ac503527d.

(8) Ang, Y. S.; Yung, L. Y. L. Rapid and Label-Free Single-Nucleotide Discrimination via an Integrative Nanoparticle-Nanopore Approach. *ACS Nano* **2012**, *6* (10), 8815–8823. https://doi.org/10.1021/nn302636z.

(9) Lan, W.-J.; Holden, D. a.; Liu, J.; White, H. S. Pressure-Driven Nanoparticle Transport across Glass Membranes Containing a Conical-Shaped Nanopore. *J. Phys. Chem. C* **2011**, *115* (38), 18445–18452. https://doi.org/10.1021/jp204839j.

(10) German, S. R.; Luo, L.; White, H. S.; Mega, T. L. Controlling Nanoparticle Dynamics in Conical Nanopores. *J. Phys. Chem. C* **2013**, *117* (1), 703–711. https://doi.org/10.1021/jp310513v.

(11) Ito, T.; Sun, L.; Henriquez, R. R.; Crooks, R. M. A Carbon Nanotube-Based Coulter Nanoparticle Counter. *Acc. Chem. Res.* **2004**, *37* (12), 937–945. https://doi.org/10.1021/ar040108+.

(12) Branton, D.; Deamer, D. W.; Marziali, A.; Bayley, H.; Benner, S. A.; Butler, T.; Di Ventra, M.; Garaj, S.; Hibbs, A.; Huang, X.; et al. The Potential and Challenges of Nanopore Sequencing. *Nat. Biotechnol.* **2008**, *26* (10), 1146–1153. https://doi.org/10.1038/nbt.1495.

(13) Clarke, J.; Wu, H. C.; Jayasinghe, L.; Patel, A.; Reid, S.; Bayley, H. Continuous Base Identification for Single-Molecule Nanopore DNA Sequencing. *Nat. Nanotechnol.* **2009**, *4* (4), 265–270. https://doi.org/10.1038/nnano.2009.12.

(14) Taniguchi, M. Selective Multidetection Using Nanopores. *Anal. Chem.* **2015**, *87* (1), 188–199. https://doi.org/10.1021/ac504186m.

(15) Theuns, S.; Vanmechelen, B.; Bernaert, Q.; Deboutte, W.; Vandenhole, M.; Beller, L.; Matthijnssens, J.; Maes, P.; Nauwynck, H. J. Nanopore Sequencing as a Revolutionary Diagnostic Tool for Porcine Viral Enteric Disease Complexes Identifies Porcine Kobuvirus as an Important Enteric Virus. *Sci. Rep.* **2018**, *8* (1), 9830. https://doi.org/10.1038/s41598-018-28180-9.

(16) Bayley, H.; Martin, C. R. Resistive-Pulse Sensing - from Microbes to Molecules. *Chem. Rev.* **2000**, *100* (7), 2575–2594. https://doi.org/10.1021/cr980099g.

(17) Sowerby, S. J.; Broom, M. F.; Petersen, G. B. Dynamically Resizable Nanometre-Scale Apertures for Molecular Sensing. *Sensors Actuators, B Chem.* **2007**, *123* (1), 325–330. https://doi.org/10.1016/j.snb.2006.08.031.

(18) Lan, W.-J.; Holden, D. a; White, H. S. Pressure-Dependent Ion Current Rectification in Conical-Shaped Glass Nanopores. *J. Am. Chem. Soc.* **2011**, *133* (34), 13300–13303. https://doi.org/10.1021/ja205773a.

(19) Chen, L.; He, H.; Jin, Y. Counting and Dynamic Studies of the Small Unilamellar Phospholipid Vesicle Translocation with Single Conical Glass Nanopores. *Anal. Chem.* **2015**, *87* (1), 522–529. https://doi.org/10.1021/ac5029243.

(20) Holden, D. A.; Watkins, J. J.; White, H. S. Resistive-Pulse Detection of Multilamellar Liposomes. *Langmuir* **2012**, *28* (19), 7572–7577. https://doi.org/10.1021/la300993a.

(21) Holden, D. A.; Hendrickson, G.; Lyon, L. A.; White, H. S. Resistive Pulse Analysis of Microgel Deformation during Nanopore Translocation. *J. Phys. Chem. C* **2011**, *115* (7), 2999–3004. https://doi.org/10.1021/jp111244v.

(22) Fraikin, J. L.; Teesalu, T.; McKenney, C. M.; Ruoslahti, E.; Cleland, A. N. A High-Throughput Label-Free Nanoparticle Analyser. *Nat. Nanotechnol.* **2011**, *6* (5), 308–313. https://doi.org/10.1038/nnano.2011.24.

(23) Davenport, M.; Healy, K.; Pevarnik, M.; Teslich, N.; Cabrini, S.; Morrison, A. P.; Siwy, Z. S.; Létant, S. E. The Role of Pore Geometry in Single Nanoparticle Detection. *ACS Nano* **2012**, *6* (9), 8366–8380. https://doi.org/10.1021/nn303126n.

(24) Willmott, G. R.; Platt, M.; Lee, G. U. Resistive Pulse Sensing of Magnetic Beads and Supraparticle Structures Using Tunable Pores. *Biomicrofluidics* **2012**, *6* (1). https://doi.org/10.1063/1.3673596.

(25) Peng, R.; Li, D. Detection and Sizing of Nanoparticles and DNA on PDMS Nanofluidic Chips Based on Differential Resistive Pulse Sensing. *Nanoscale* **2017**, *9* (18), 5964–5974.

https://doi.org/10.1039/c7nr00488e.

(26) Ang, K. H. A. K. H.; Chong, G.; Li, Y. L. Y. PID Control System Analysis, Design, and Technology. *IEEE Trans. Control Syst. Technol.* **2005**, *13* (4), 559–576. https://doi.org/10.1109/TCST.2005.847331.

(27) Foley, T. M. A Study of Acoustic Cavitation and Hydrogen Production, University of Southampton, 2015.

(28) Anderson, J. L.; Quinn, J. A. The Relationship between Particle Size and Signal in Coulter-Type Counters. *Rev. Sci. Instrum.* **1971**, *42* (8), 1257–1258. https://doi.org/10.1063/1.1685356.

(29) Smythe, W. R. Flow around a Spheroid in a Circular Tube. *Phys. Fluids* **1964**, *7* (5), 633–638. https://doi.org/10.1063/1.1711260.

(30) Birkin, P. R.; O'Connor, R.; Rapple, C.; Martinez, S. S. Electrochemical Measurement of Erosion from Individual Cavitation Events Generated from Continuous Ultrasound. *J. Chem. Soc. Faraday Trans.* **1998**, *94* (July), 3365–3371.

(31) Birkin, P. R.; Silva-Martinez, S. The Effect of Ultrasound on Mass Transfer to a Microelectrode. *J. Chem. Soc. Chem. Commun.* **1995**, 1807–1808.

(32) Frankel, G. S.; Jahnes, C. V; Brusic, V.; Davenport, A. J. REPASSIVATION TRANSIENTS MEASURED WITH THE BREAKING-ELECTRODE TECHNIQUE ON ALUMINUM THIN-FILM SAMPLES. *J. Electrochem. Soc.* **1995**, *142* (7), 2290–2295.

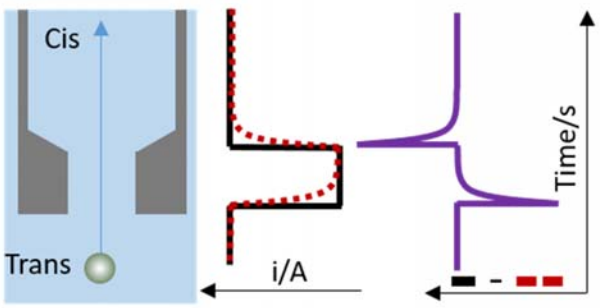
Cis
Trans
i/A
Time/s